MARHS: Mobility Assessment System with Remote Healthcare Functionality for Movement Disorders

Sunghoon Ivan Lee*, Jonathan Woodbridge*, Ani Nahapetian*†, Majid Sarrafzadeh*
*Computer Science Department
University of California Los Angeles
Los Angeles, USA
†Department of Computer Science
California State University Northridge
Northridge, USA
silee@cs.ucla.edu, jwoodbri@cs.ucla.edu, ani@csun.edu, majid@cs.ucla.edu

ABSTRACT

Due to the global trend of aging societies with increasing demand for low cost and high quality healthcare services, there has been extensive research and development directed toward wireless and remote healthcare technology that considers age-associated ailments. In this paper, we introduce Mobility Assessment and Remote Healthcare System (MARHS) that utilizes a force sensor in order to provide quantitative assessment of the mobility level of patients with movement disorder ailment, which is one common age-associated ailment. The proposed system also enables the remote healthcare services that allow patients to receive diagnoses from clinical experts without his/her presence. MARHS also contains a data analysis unit in order to provide information that summarizes the characteristics of symptoms of a group of patients (e.g., patients with a certain type of ailment) using a combination of feature ranking, feature selection, and classification algorithms. The results of the analyses on the data from a clinical trial show that the examination results of the proposed system can accurately recognize various groups of patients, such as, patients with (i) chronic obstructive pulmonary disease, (ii) hypertension, and (iii) cerebral vascular accident with an average accuracy of 90.05%, 82.60%, and 93.54%, respectively.

Categories and Subject Descriptors

C.3 [**Special-Purpose and Application-based Systems**]; H.4 [**Information Systems Applications**]: Miscellaneous

General Terms

Measurement, Design, Performance, Experimentation, Human Factors

Keywords

Remote health, movement disorders, force sensors.

Permission to make digital or hard copies of all or part of this work for personal or classroom use is granted without fee provided that copies are not made or distributed for profit or commercial advantage and that copies bear this notice and the full citation on the first page. To copy otherwise, to republish, to post on servers or to redistribute to lists, requires prior specific permission and/or a fee.
IHI'12, January 28–30, 2012, Miami, Florida, USA.
Copyright 2012 ACM 978-1-4503-0781-9/12/01 ...$10.00.

1. INTRODUCTION

In the United States, the number of older adults is expected to reach 71 million, or roughly 20% of the population, by 2030 [1, 23]. As a result of the worldwide trend towards aging societies, the care for ailments associated with the elderly, such as Alzheimer disease, diabetes, and Parkinson's diseases (PD), is expected to be in high demand. We are particularly interested in movement disorder ailments such as PD, stroke, arthritis, and tremor, the most common age-associated ailments [5]. Movement disorders affect the function of motor neurons and, thus, restrict the movement of the body, including upper limbs, gait and speech. Modern medical treatments for movement disorders are combinations of medication, surgical operation, and rehabilitation. In order to investigate the consequences of these medical treatments, a method to measure the motor performance of patients is often required.

Currently, the ailment progress or rehabilitation performance are assessed by physicians based on observation of the patient's motor performance [10, 7], which makes the measurement subjective and based on limited ordinal scales [13, 7]. This creates a need for quantitative assessment methods, such that the analysis of a patient's motor performance can be made more accurate and objective [8, 13]. Moreover, the current assessment systems for movement disorder ailments require the presence of a physician and demand high-priced services. Due to dramatic advances in recent telecommunications and information technology, remote health systems are considered as solutions that provide quality healthcare services at low costs. Telehealth or remote health systems are defined as the application of telecommunications and information technology to the delivery of healthcare, health related services, and health related information beyond physical boarders [16, 4].

In this paper, we introduce Movement Assessment and Remote Healthcare System (MARHS). This system provides accurate and quantitative measurements of handgrip performance of patients with movement disorder ailments. We utilize the handgrip performance of patients to reflect the level of mobility because handgrip strength is known as a simple, accurate, and economical bedside measurement of muscle function and the progression of the movement disorders [13, 6, 15, 17, 19, 20, 11, 18, 14]. MARHS also provides remote healthcare services by supporting rich data analysis on patient's handgrip performance such that physicians and medical professionals can make diagnoses remotely. The data analysis unit (DAU) of the proposed system shows that the resulting signals provide valuable information reflecting

the condition of the patient's ailment. In order to address this, the DAU recognizes and classifies signals of a particular group of interest (e.g., a patient with a particular ailment) from other signals. By successfully classifying signals of a group of interest, we show that the resulting signals of MARHS contain important information defining the characteristics of that group (i.e., a particular ailment). Moreover, the DAU provides information about features that contribute the most in the classification process, which can be used to define the ailment characteristics of the interested group of patients. The numeric values of these features can be used to provide quantitative measurements of the level of mobility. The DAU utilizes a combination of feature ranking, feature selection, and classification mechanisms in order to address the aforementioned tasks.

This paper presents data analysis results of the proposed system based on data collected from a clinical trial performed at St. Vincent Hospital in Los Angeles, California, USA.

This paper is organized as follows. Section 2 discusses the related works. Section 3 introduces the hardware and software architecture design of the proposed system. In Section 4, the DAU of the proposed system is discussed in detail. Section 5 presents data analysis results using data collected from a clinical trial. Finally, conclusion and future work is discussed in Section 6 and 7, respectively.

2. RELATED WORKS

Many studies examined embedded systems for assessing handgrip strength [10, 6, 15]. The system introduced in [10] monitors the muscle activities using force sensors on the palm and digits. In [6], a system that monitors the grip strength and the digit muscle activities is introduced. Moreover, in [15], an embedded system that assesses the grip force behavior during object manipulation is introduced. The proposed work, unlike the aforementioned works, not only introduces an embedded system that efficiently monitors the grip performance, but also discusses how the examination results can be processed to correlate to the subjects' ailment conditions using data from a clinical trial.

In [11], authors investigate the handgrip strength and endurance of healthy subjects and patients, and conclude that handgrip strength and mobility for patients are strongly correlated. They measure handgrip strength, endurance, and work, and perform one-to-one comparisons between each measurement and mobility. In other words, the authors assume that the measurements are independent of each other and, thus, correlation between the combination of those measurements and mobility is not considered. On the other hand, our system considers the correlation between various combinations of multiple features and the patient's disease condition. Additionally, the system proposed in [11] can only process features (i.e., strength, endurance or work) that are pre-defined, but the proposed system allows users to add or remove features from a feature pool and intelligently selects features that are useful to characterize a certain group of patients. Moreover, and most importantly, our work presents a system that allows remote healthcare services integrated with assessment of handgrip performance.

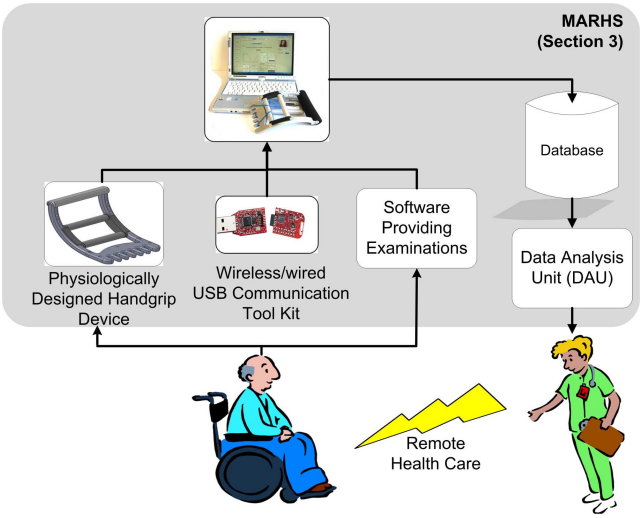

Figure 1: The graphical overview of the proposed system. A patient is examined based on various tests provided by the software and the handgrip device. The results are transmitted to a computer using a communication tool kit and stored in a database. The examination results and the data analysis results can be remotely accessed by clinical experts.

3. MOVEMENT ASSESSMENT AND REMOTE HEALTHCARE SYSTEM (MARHS)

The objective of the system is to provide handgrip examinations, retrieve signals from subjects, store the results in the database, and finally analyze the signals in the database in order to provide information such as features that characterizes patients' ailment symptoms. An overview of the proposed system is illustrated in Figure 1. The proposed system can be divided into two subsystems: the hardware system and the software system. The hardware system contains physical devices such as the handgrip device, the force sensor, and the communication device. The major objective of the hardware system is to collect the time-varying grip strength of the patient and to send the data stream to the software system. The software system communicates with the hardware system in order to store the examination results in the database, and perform the data analysis on the results. We discuss the detailed system architecture for both the hardware and software system in Section 3.1 and 3.2, respectively.

3.1 Hardware Architecture

3.1.1 Handgrip Device

The handgrip device of MARHS is based on medical devices used by clinical professionals (e.g., handgrip device in [22]), as shown in Figure 2. Our device is composed of 6061 t-6 Aluminum and Delrin plastic, which are lightweight and rigid. The black plastic component of the handgrip device is composed of Delrin plastic. The two cylinders bridged by the black plastic (Part-C in Figure 2 (a)) are movable along the sideline (Part-B in Figure 2 (a)) such that patients can grasp the device. The movable component of the handgrip

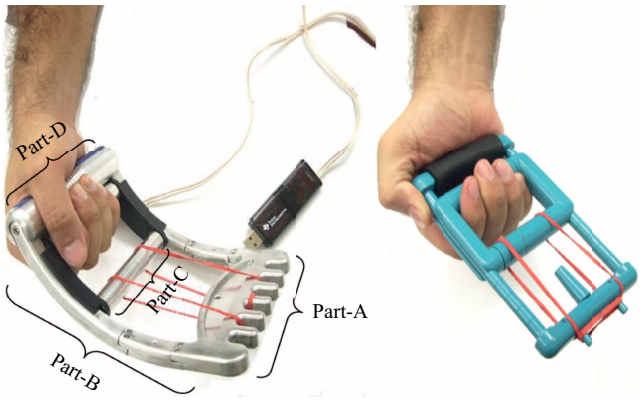

Figure 2: (a) The physiologically designed handgrip device of MARHS (left) and (b) the handgrip device currently in use (right)

device is bound to the fork-like side (Part-A in Figure 2 (a)) of the handgrip by a rubber band. Patients can use rubber bands of different tension force in order to customize the squeeze force in the handgrip device. Additionally, the fork-like side of the handgrip allows patients to further adjust the tension force by placing the rubber band at different widths. Note that patients can adjust the initial position of the movable component of the handgrip device by using adjustable pin holes on the sideline (i.e., Part-B in Figure 2 (a)) of the handgrip. Thus, grasping performance of various patients with different size of extremities can be optimized. Finally, a force sensor is attached to Part-D in Figure 2 (a), and it measures the force generated from the grasping action.

3.1.2 Force Sensors

In MARHS, a force sensor is attached to the handgrip device in order to measure the grip strength. We employ a commercial FSR™ sensor (Interlink Electronics, Camarillo, CA, US) [2] in our system. The FSR sensor is a thin-film force sensor that contains a thermoplastic sheet and a conductive polyetherimide film facing to each other [21]. When there is no force applied to the FSR sensor, the two sheets are electrically separated, which generates infinite impedance. In the case when there is a force applied to the sensor, the two sheets make electrical contact, and finite impedance is generated. As the amount of force applied increases, the resistance generated by the FSR sensor decreases [21]. We employ the FSR sensors in the proposed system because (i) the FSR sensor responses accurately and precisely to the general range of handgrip force, and (ii) the FSR shows good performance in terms of robustness [21].

3.1.3 Communication Port

The communication device delivers the pressure values captured by the force sensor to the software (Section 3.2). In our proposed system, an MSP430 (Texas Instruments, Dallas, Texas, USA) [3] is employed as the communication device. The MSP430 is a communication device that allows the force sensor on the handgrip device to communicate with the software either in wired or wireless manner. The MSP430 uses USB as its communication port at the receiver-side. The modulation rate is 9600 symbols per second with each symbol being 8-bits long. The MSP430 contains a Micro Controller Unit that allows us to implement software using a simple handshake mechanism in order to initiate and terminate the communication. This dramatically decreases the required power when the device is communicating wirelessly.

3.2 Software Architecture

The examinations provided by the software are designed such that a patient's grip strength as well as the preciseness of a patient's ability to control the grip strength can be effectively measured. Due to the various physical conditions of different patients, patients have different handgrip strength. Thus, the examinations must be normalized based on physical conditions of different patients. In order to solve the problem, the system measures the maximum voluntary contraction (MVC) and normalizes the examination based on the value of MVC for each patient. MVC defines that a patient voluntarily grasps the handgrip device with his/her maximum effort.

Patients may proceed to the actual examination followed by the calibration process. Figure 3 (a) illustrates an example of an examination using a sinusoidal waveform. When the examination begins, the target waveform (red line) is horizontally shifted to the left at a constant speed, and thus, users observe a flow of the waveform within the screen. The blue circle in the middle of the screen corresponds to the level of pressure acquired from the force sensor. The blue circle is always located in the middle of the x-axis and its position in the y-axis changes according to the pressure provided by the patient. The labels on y-axis represent the percentage of the acquired pressure compared to the MVC measured in the calibration process. The objective of the examination is to control the grip strength, so that the blue circle can be overlapped to the waveform as much as possible. In summary, the examination considers both the maximum strength and the preciseness of patients' grip control.

The software provides different waveforms including the sinusoidal waveform such as exponential and step-function waveform. Moreover, the software provides a number of test parameters, which may change the attributes of the test. For example, patients may change the speed of the waveform horizontally shifting or the size of the blue circle, which allows patients to perform the test at different levels of difficulties. Additionally, users may vary the time duration of the test.

The result waveforms created by the patients and the annotative information are stored in the database system in order to deliver maximum range of information about the examination. The information stored in the database system can be remotely retrieved by physicians or clinicians for quality remote healthcare services. Figure 3 (b) illustrates an example of this remote healthcare functionality. This interface also allows physicians to provide various inputs to the DAU (Section 4), and to retrieve the results from the DAU including information such as unique symptoms of a particular ailment.

The software is programmed in C# .NET and the database system is designed in SQL.

4. DATA ANALYSIS UNIT

In this section, we introduce the DAU, which extracts important information from the patient-generated signals and

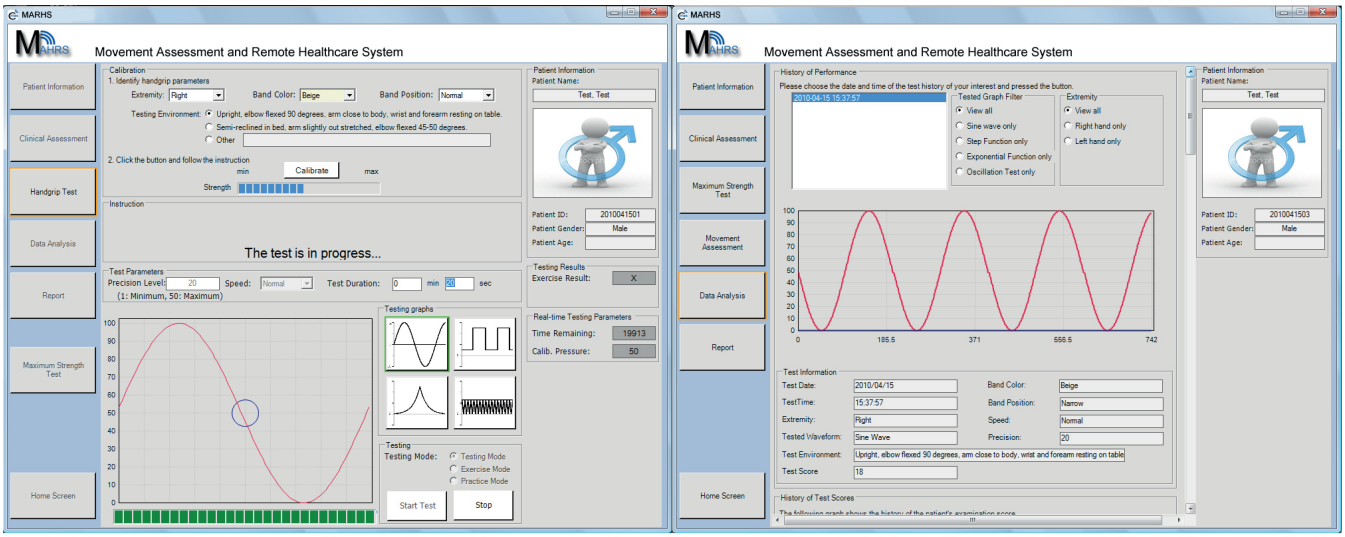

Figure 3: Screenshots of the software of MARHS. Screenshot in (a) illustrates an example of an examination on handgrip performance, and screenshot in (b) illustrates an example of the remote healthcare functionality of MARHS, which allows physicians to retrieve clinical and examination information stored in the database.

summarizes the characteristics of symptoms of patients. In order to address this objective, we employ a feature ranking mechanism, a feature selection mechanism, and a classification algorithm. We classify signals from a group of patients of particular interest. By successfully classifying signals of interest from other signals, we show that the signals generated by MARHS contain valuable information, which may reflect the characteristics of the selected group of patients. Thus, it allows us to further process the signals to quantify multiple aspects of patients' mobility levels. Additionally, the DAU provides information about subset features that contribute the most in the classification process using feature ranking and feature selection mechanism. These features may characterize unique symptoms of patients of our particular interest.

4.1 Software Interface

The prototype interface of the DAU is illustrated in Figure 4. The DAU begins with forming a group of signals of interest. Throughout this paper, we generically use the term *group of interest* (GOI) to represent the signals in which we are particularly interested to analyze. The software interface asks users to define the GOI by checking the checkbox as shown in Figure 4, which is used as the ground truth label in order to evaluate the classification performance. The GOI can be flexibly defined in order to characterize different sets of the examination results. For example, we can define the GOI as the signals of patients with Cerebral Vascular Accident (CVA) and compare these signals against the signals of patients without CVA. If we can successfully classify signals of patients with CVA from other patients, we can claim that the resulting signals of MARHS contain information (i.e., features), which may define characteristics of patients with CVA. Note that we also use the term *positive signals* and *negative signals* to define the signals in the GOI and the signals in the complement of the GOI, respectively. The DAU interface then allows users to add, delete and modify feature functions to be considered in the feature selection and classification process. Finally, the DAU interface displays the data analysis results when users press a command button. The flow of signals in the DAU is illustrated in Figure 5. Each component in Figure 5 is further discussed in the following subsections.

4.2 Feature Extraction

The DAU starts the data analysis process by extracting features from the examination results. Suppose that we represent a vector of extracted features from a single examination result as

$$\overline{s} = \begin{bmatrix} s_1 & s_2 & \cdots & s_T \end{bmatrix}, \tag{1}$$

where T is the number of features. We further suppose that $w_g[n]$ represents the target waveform (e.g., perfect sinusoidal waveform) and $w_r[n]$ represents the waveform generated by the patient (e.g., the trajectory of the blue circle in Figure 3 (a) over a period of time). Then each feature s_i can be represented as a function of $w_g[n]$ and/or $w_r[n]$,

$$s_i = f_i\left(w_g[n], w_r[n]\right).$$

We define $f_i(\cdot)$ as a feature extraction function, which is either in time-domain or in frequency-domain. An example of feature extraction functions in time-domain can be the average difference between the magnitude of $w_g[n]$ and $w_r[n]$. This example of the feature extraction function can be mathematically expressed as

$$f = \frac{1}{N}\sum_{n=1}^{N} |w_g[n] - w_r[n]|, \tag{2}$$

where N is the length of $w_g[n]$ and $w_r[n]$. An example of feature extraction functions in frequency-domain can be the magnitude of harmonics at the frequency range between 3 to 6 Hz (patients with Parkinson's disease are known to have

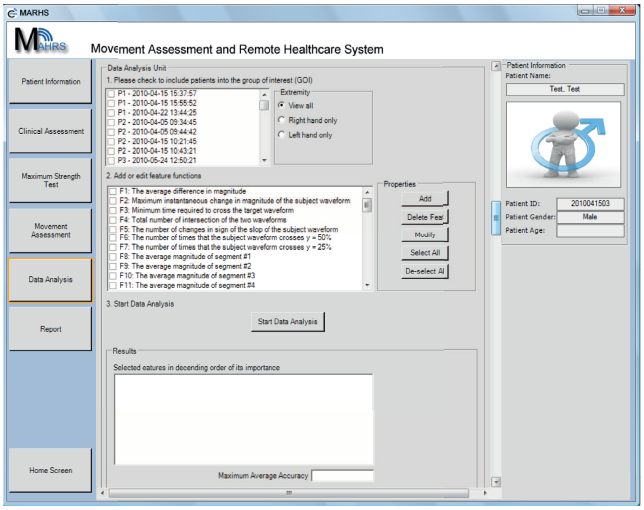

Figure 4: A screenshot of the software interface of the DAU. This prototype interface allows users to define a group of signals of interest (i.e., a particular ailment) and feature functions to be considered in the analysis. The system displays the results upon users' requests.

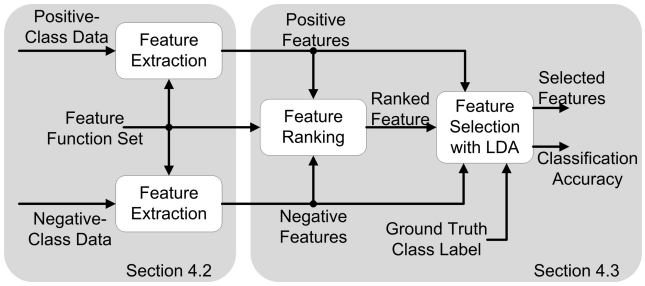

Figure 5: The graphical overview and data flow of the DAU. The DAU extracts identical features from both positive and negative class data. Then, the DAU performs wrapper approach to select important features based on the results of the feature ranking and classification (LDA).

tremors of frequency around 3 to 6 Hz). This function can be mathematically expressed as

$$f = \sum_{k \in [3-6Hz]} |W_r[k]|, \tag{3}$$

where $W_r[k]$ is the Discrete Fourier Transform (DFT) of $w_r[n]$. Note that the formal example of the feature selection function is a linear function and the latter example is a non-linear function.

Once a set of feature extraction functions is defined, we extract features from all signals. Suppose that M represents the total number of signals including both positive and negative signals. Then, we can extracts total M number of arrays of features, which can be represented as a two dimensional array,

$$S = \begin{bmatrix} \overline{s}^1 \\ \overline{s}^2 \\ \vdots \\ \overline{s}^M \end{bmatrix} = \begin{bmatrix} s_1^1 & s_2^1 & \cdots & s_T^1 \\ s_1^2 & s_2^2 & \cdots & s_T^2 \\ \vdots & & \ddots & \vdots \\ s_1^M & s_2^M & \cdots & s_T^M \end{bmatrix} \tag{4}$$

$$= \begin{bmatrix} \overline{s}_1 & \overline{s}_2 & \cdots & \overline{s}_T \end{bmatrix}, \tag{5}$$

where $\overline{s}^j$ with $j \in [1, M]$ is a horizontal array of features as in (1) and $\overline{s}_i$ with $i \in [1, T]$ is a vertical array composed of values of a feature $f_i(\cdot)$ computed from the entire signals.

4.3 Feature Selection and Classification

The DAU runs a feature selection technique based on an instance of the wrapper approach. The wrapper approach determines a set of features that have small contribution in classifying data based on the results of the feature ranking technique [9, 12]. Feature ranking technique is a metric to evaluate the performance of a feature in the classification process. The reason that we employ feature ranking and feature selection techniques are as follows. First, given a pre-defined set of features as in (1), not all of these features play important role in classifying a certain GOI. This may lead to a problem during the classification process that a collection of many useless features can be accumulated to overwhelm some useful features (i.e., overfitting problem). Second, it is more efficient computationally since it filters out features that are less useful. Lastly, information about the rank of features according to the level of contributions in the classification process is valuable to us because features with higher rank can be defined as unique symptoms found only in that GOI. In MARHS, we employ the estimated Pearson correlation coefficients to rank the features according to the level of correlation to the class labels (i.e., positive or negative signals). The Pearson correlation coefficient for a feature f_i, can be estimated using

$$R(i) = \frac{\sum_{j=1}^{M} \left(s_i^j - E(\overline{s}_i)\right)\left(y^j - E(\overline{y})\right)}{\sqrt{\sum_{j=1}^{M} \left(s_i^j - E(\overline{s}_i)\right)^2 \sum_{j=1}^{M} \left(y^j - E(\overline{y})\right)^2}}, \tag{6}$$

where y^j with $j \in [1, M]$ represents the class of the signal j (i.e., $+1$ for positive and -1 for negative class signal) and $E(\cdot)$ represents a function computing the mean value of the input vector. Then, we use $R(i)^2$ as a feature ranking criterion that estimates goodness of linear fit of an individual feature to the class vector $\overline{y}$ [9].

Given the rank of all features, the wrapper approach needs to decide (i) how to construct the subset feature search space and (ii) which classification algorithm to be used to assess the performance of different subset features. The simplest search space is to consider all possible feature combinations and perform the chosen classification algorithm to evaluate the performance for each feature combination. However, for T features, the evaluation must be performed for $2^T - 1$ combinations, which is not computationally feasible. Thus, we utilize the famous *forward selection* strategy to construct the search space, which starts with the highest ranked feature and gradually adds a feature that is the next highest ranked. Then, the size of the search space is reduced to $T - 1$. In order to evaluate each feature subset, we utilize leave-one-out cross validation with Linear Discriminant Analysis (LDA) as the classification algorithm. Each feature subset is evaluated using the average classification accuracy based on leave-one-out cross validation. Algorithm 1 shows the pseudo-code for the feature selection algorithm used in the DAU.

Algorithm 1 Wrapper approach feature selection algorithm using forward selection

$F = [f_1, f_2, \cdots, f_T]$ {entire feature sets sorted in a decreasing order of feature ranking from (6)}
S {M by T data matrix as in (4)}
$\overline{y}$ {M by 1 matrix of classes as in (6)}
$V = [\phi]$ {array that will contain average classification accuracy of each feature subset}
for $i = 1$ to T **do**
  $F = F[1:i]$ {selecting the most significant i features}
  $A = [\phi]$
  for $j = 1$ to M **do**
    $S^{'} = S - \overline{s}^j$ {leave-one-out training set}
    $\overline{y}^{'} = \overline{y} - y^j$ {class label for training set}
    $X^{'} = S^{'}[:, F]$ {considering subset feature}
    $\theta = \text{LDA}\left(X^{'}, \overline{y}^{'}\right)$ {training}
    $y^* = \theta * s$ {predicted class of the testing set $\overline{s}^j$}
    if $y^* == y^j$ **then**
      $A[j] = 1$ {correctly classified}
    else
      $A[j] = 0$ {incorrectly classified}
    end if
  end for
  $V[i] = E(A)$ {computing the average classification accuracy}
end for
$n = \arg\max_i V[i]$
return $[f_1, f_2, \cdots, f_n]$ {subset of features producing the maximum accuracy}

4.4 Other Feature Ranking and Classification Methods

In addition to Pearson correlation coefficient, we tried a number of different feature ranking methods such as information theoretic approach or single-feature classification approach. We also tried different classification algorithms such as Naive Bayes, decision tree, support vector machine (SVM), and adaptive boost (AdaBoost) instead of LDA. However, any combination of the aforementioned methods did not show any superior performance compared to the proposed combination of Pearson correlation method and LDA.

5. CLINICAL TRIAL AND DATA ANALYSIS

This section presents the data analysis results of our system including the DAU based on data obtained from a clinical trial of the proposed MAHRS, performed at St. Vincent Medical Center (Los Angeles, CA). A total of 12 patient subjects participated in this clinical trial. The clinical information about patient subjects is provided in Table 1. All patients were examined under the same environment such that the examination results are not affected by factors other than the mobility performance of subjects. For example, each subject performed the examination while he/she was seating upright, had elbow flexed 90 degrees with arm close to the body, and had wrist and forearm resting on a table. Note that all subjects had performed the test using the sinusoidal waveform as the target waveform with test duration of 20 seconds in order to make the results comparable to each other.

This data analysis considers three different GOIs: (i) a group of patients with Chronic Inflammatory Demyelinating Polyneuropathy (CIDP), (ii) a group of patients with hypertension, and (iii) a group of patients with Cerebral Vascular Accident (CVA). These three GOIs are chosen among various ailments described in Table 1 such that each GOI can be analyzed with a sufficient number of signals. For example, a total of 24 signals are available for patients diagnosed with CIDP (Patient Subjects 6 and 8), a total of 25 signals for hypertension (Patient Subjects 1, 3, 4, and 5), and a total of 17 signals for CVA (Patient Subjects 3, 7, 10, and 12). Ailments such as Parkinson's disease or diabetes are not considered because the number of available signals is too small to be used to train and test the system. Figure 6 illustrates sample examination results of the three GOIs that we consider in this analysis. The target waveform (i.e., perfect sinusoidal waveform) is depicted by the red dotted line, and the patient generated waveform is depicted by the blue solid line. Figure 6 (a) illustrates sample signals of patients with CIDP, Figure 6 (b) illustrates samples of patients with hypertension, and Figure 6 (c) illustrates samples of patients with CVA.

5.1 Feature Pool

This section presents features used in the data analysis in order to define the characteristics of different GOIs. A total of 45 candidate feature functions are defined: 36 functions extracts features in the time-domain and 9 functions in the frequency domain. These features are further analyzed as explained in Section 4, and a subset of these 45 features is selected to define the characteristics of the tested GOI. The feature functions are denoted as f_i with $1 \leq i \leq 45$, where the first 36 feature functions are in the time-domain and the following 9 feature functions are in the frequency-domain. The first time-domain feature extraction function, denoted as f_1, is based on the average difference in magnitude between the target waveform and the waveform generated by the subject, similar to the equation defined in (2). This function provides the overall level of performance in term of accuracy. f_2 computes the maximum instantaneous change in magnitude of the subject-generated waveform in order to investigate how well a subject manipulates the grip strength. f_3 computes the minimum time required for the subject-generated waveform to cross the target waveform from the time that the examination begins. This function provides possible information about reaction time for the subject to restore to the target waveform from deviation. The fourth time-domain function, f_4, computes the total number of intersections of two waveforms in order to investigate a subject's ability in order to control the grip strength to stay near the target waveform. f_5 investigates the number of changes in sign of the slope of the patient-generated waveform in order to correlate the examination results to possible effect of tremor. f_6 and f_7 compute the number of times that the subject-generated waveform crosses horizontal lines at magnitude y = 50% and y = 25%, respectively. The time-domain functions from f_8 to f_{22} are constructed as the following. The 20 second-long waveforms generated by subjects are quantized into 15 segments of uniform length in time axis (i.e., each segment contains the data of 20/15 seconds). Then, f_8 to f_{22} contain the mean

Table 1: Limited clinical information about patient subjects tested on the proposed system. The last column (i.e., Number of tests) provides the number of tests performed for each subject. Note that associated diseases of Patient Subject 2, 10, and 11 are not provided due to the participants' unwillingness to reveal their information (N/A stands for Not-Available). However, this unrevealed information does not complicate any of the data analysis results provided Section 5.2, 5.3, and 5.4.

	Age	Gender	Primary diagnosis	Secondary diagnosis	Number of tests
Patient Subject 1	85	Male	Arthritis Left Hip	Hypertension	8
Patient Subject 2	49	Female	N/A	-	3
Patient Subject 3	87	Female	Cerebral Vascular Accident	Hypertension	6
Patient Subject 4	73	Male	Chronic Obstructive Pulmonary Disease	Hypertension	4
Patient Subject 5	72	Male	Intra-Cranial Hemorrhage	Hypertension / Diabetes	7
Patient Subject 6	73	Male	Fracture L Tibia	Chronic Inflammatory Demylenating Polyneuropathy	6
Patient Subject 7	65	Female	Progressive Debility	Multiple CVA	3
Patient Subject 8	73	Male	Chronic Inflammatory Demylenating Polyneuropathy	Hypotension/Pancytopenia	18
Patient Subject 9	74	Male	Parkinson's Disease	-	2
Patient Subject 10	60	Male	N/A	CVA	4
Patient Subject 11	74	Female	N/A	-	2
Patient Subject 12	61	Female	NTBI	CVA	4

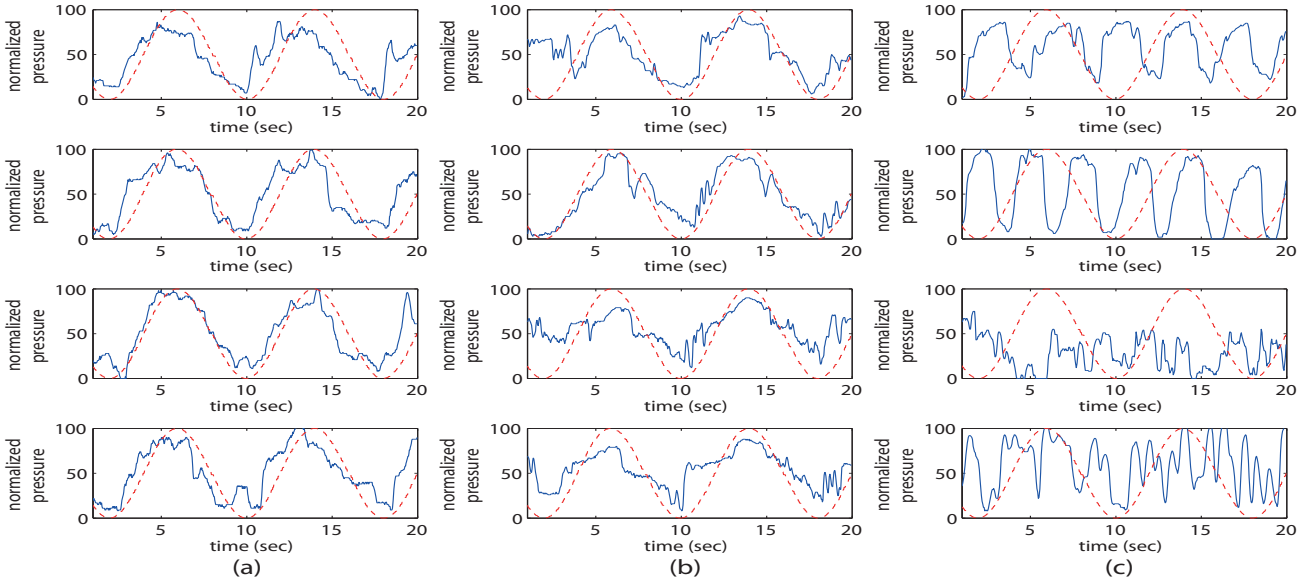

Figure 6: Sample signals of subjects with various conditions. The four signals in column (a) belong to patients with CIDP (the top two signals from Patient Subject 6 and the bottom two from Patient Subject 8 in Table 1). The signals in column (b) belong to patients with hypertension (one from each Patient Subjects 1, 3, 4, and 5). The signals in column (c) are sample signals from patients with CVA (one from each Patient Subjects 3, 7, 10, and 12).

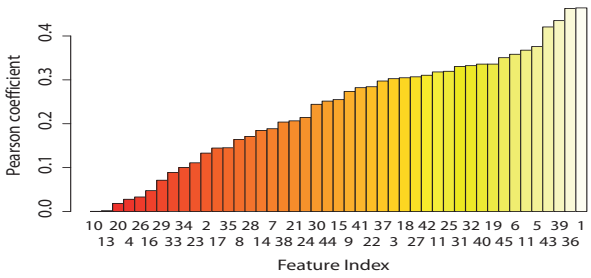

Figure 7: The ranking (Pearson coefficients) of features for GOI composed of patients with CIDP. The results show that f_1 (the right-most index) provides the highest correlation to CIDP and f_{10} (the left-most index) provides the lowest correlation.

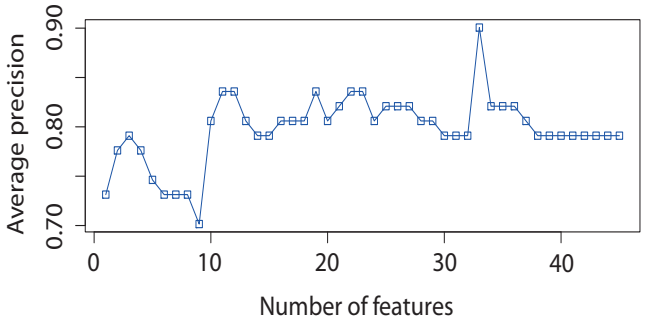

Figure 8: The average classification accuracy of GOI composed of patients with CIDP over the search space using forward selection strategy. The results show that the maximum average accuracy of 90.05% is achieved when the highest 33 features are employed.

values of the magnitude of these segment. These quatized segments are used to evaluate the changes in grip strength over time. Furthermore, the time-domain functions from f_{23} to f_{36} compute the difference in mean magnitude of the two neighboring segments. These features are used to evaluate how fast the grip strength of a patient changes over time. The frequency-domain functions used in this analysis are computed as the following. The first frequency-domain function, f_{37}, computes the average difference in magnitude between the DFT of the target waveform and the DFT of the subject-generated waveform over all possible frequency range. The frequency-domain functions from f_{38} to f_{45} divide frequency range from 0 Hz to 16 Hz into 8 segments of uniform length (i.e., 2 Hz), and compute the spectrum energy for each segment in order to investigate the tremor effect at various frequency ranges.

5.2 Patients with CIDP

This section presents the data analysis results when the GOI is defined as the signals of patients with CIDP. In other words, we define the positive-class data as the signals of Patient Subjects 6 and 8 in Table 1, and the negative-class data as the signals of the rest of patients. Some sample signals in the positive class are provided in Figure 6 (a). As discussed in Section 4, the extracted features from both positive and negative classes are evaluated using equation (6). Note that M in (6) represents the total number of signals considered in this analysis (i.e., $M = 67$) and T represents the total number of features (i.e., $T = 45$). Moreover, $y^j = 1$ if the j^{th} signal belongs to the GOI and $y^j = 0$ otherwise. The evaluated feature ranking for this analysis is provided in Figure 7, where the feature functions are sorted in an increasing order of their ranking. According to the graph, f_1 has the highest correlation to the class label $\overline{y}$ and f_{10} has the lowest correlation. As shown in Algorithm 1, we employ forward selection strategy to construct the search space. We initially start with a single feature with the highest rank (i.e., f_1), and gradually add the next highest ranked feature until we consider the entire set of features (i.e., f_1, f_2, $\cdots$, f_{45}). Figure 8 shows the average classification accuracy ($V[i]$ in Algorithm 1) over the search space (i.e., number of features in forward selection strategy). The results show that the maximum accuracy of 90.05% is achieved when the highest 33 features are employed. This implies that the classifier could successfully recognize signals of patients with CIDP at the maximum rate of 90.05%. Moreover, the highest 33 features are the distinct and unique features of patients with CIDP, which makes their signals most distinguishable from other patients. In Table 2, we provide information about the first 5 features out of the selected 33 features. Detail descriptions about these features are provided in Section 5.1.

Table 2: Summary of the first 5 features of the selected 33 features for the GOI composed of patients with CIDP

Rank	Label	Pearson coefficient
1	f_1	0.46404
2	f_{36}	0.46272
3	f_{39}	0.43509
4	f_{43}	0.42060
5	f_5	0.37586

5.3 Patients with Hypertension

A similar analysis has been conducted on the GOI composed of patients with hypertension (i.e., Patient Subjects 1, 3, 4, and 5). Some sample signals of hypertension are provided in Figure 6 (b). As discussed in Section 4, the extracted features are evaluated using equation (6). Note that the class label vector $\overline{y}$ is different from that of the previous section, since $y^j = 1$ when j^{th} signal belongs to patients with hypertension, and $y^j = 0$ otherwise. The evaluated feature ranking of this GOI is provided in Figure 9. Figure 9 shows that f_6 provides the highest correlation to the class label vector $\overline{y}$, and f_8 provides the lowest correlation. Moreover, we compute the average accuracy of classifying the patients with hypertension based on leave-one-out cross validation as explained in Algorithm 1. Figure 10 shows the average accuracy over possible search space using forward selection strategy. The maximum average accuracy is 82.60%, and this accuracy is achieved when the highest 2 features are employed. This implies that the signals of patients with hypertension could be successfully distinguished from other patients at the maximum average rate of 82.60%. Moreover, the selected features, f_6 and f_7, are the two unique features

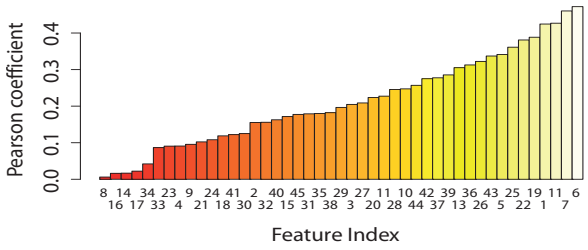

Figure 9: The ranking (Pearson coefficients) of features for GOI composed of patients with hypertension. The results show that f_6 (the right-most index) provides the highest correlation to hypertension and f_8 (the left-most index) provides the lowest correlation.

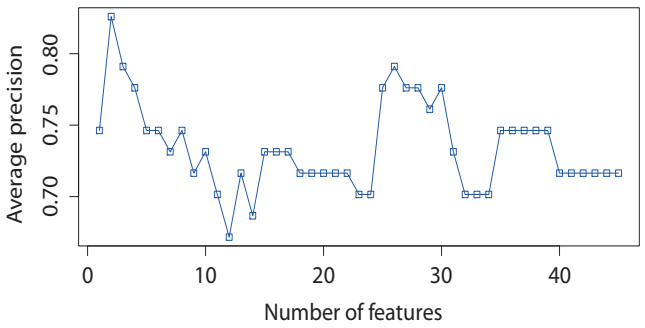

Figure 10: The average classification accuracy of GOI composed of patients with hypertension over different number of features. The results show that the maximum average accuracy of 82.60% is achieved when the highest 2 features are employed

that characterize patients with hypertension, which makes their signals the most distinguishable.

5.4 Patients with CVA

This section shows the data analysis results of MARHS when the GOI is defined as signals of patients with CVA. In other words, signals of Patient Subjects 3, 7, 10, and 12 are labeled as positive signals and the signals of the rest of patients are labeled as negative. Some sample signals of patients with CVA are shown in Figure 6 (c). The features defined in Section 5.1 are evaluated based on equation (6), and the results are displayed in Figure 11. This figure shows that f_{36} has the highest correlation with CVA, and f_9 has the least correlation. The average classification accuracy for CVA is computed in the search space created by forward selection. The results are displayed in Figure 12. It shows that the maximum average accuracy is 93.54%, and the highest 2 features are used. This implies that the signals of patients with CVA could be successfully recognized from other patients at the maximum average rate of 93.54%. Moreover, the highest two features, f_{36} and f_{39}, are the distinct and unique features that characterizes patients with CVA, which makes their signals most distinguishable.

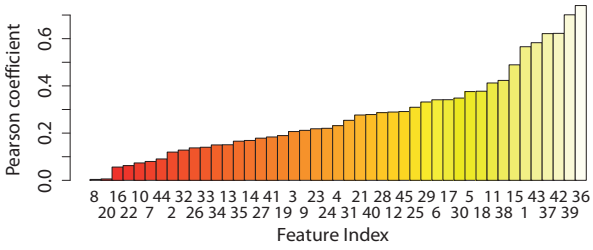

Figure 11: The ranking (Pearson coefficients) of features for GOI composed of patients with CVA. The results show that f_{36} (the right-most index) provides the highest correlation to CVA and f_8 (the left-most index) provides the lowest correlation.

6. CONCLUSION

This paper presents the Mobility Assessment and Remote Healthcare System (MARHS), which provides quantitative measurements on handgrip performance for patients with movement disorders. MARHS also provides remote healthcare services by allowing the patients to receive diagnoses from clinical experts remotely. We discussed the hardware and software architecture of the system. We also introduced the DAU, which shows that the examination results of MARHS contain information reflecting the characteristics of various ailments. In other words, examination results produced by MARHS can be used to diagnose the disease progress or condition of a patient and, thus, quantitative measurements computed based on these examination results can provide valuable information. We have performed three data analysis using signals that we acquired from a clinical trial at St. Vincent Medical Center (Los Angeles, CA). The first analysis was to classify signals of patients with CIDP, and we achieved the maximum average classification accuracy of 90.05%. We also performed analyses to classify signals of patients with hypertension and CVA, and we achieved the maximum average accuracy of 82.60% and 93.54%, respectively. These results, which show high classification accuracy, help us to conclude that the examination results of MARHS may be utilized as a metric to quantify the disease progress and condition of a patient.

7. FUTURE WORK

There exist many potential research directions that we can be pursued in the future. We can perform experiments showing the correlation between the examination results and the effectiveness of a certain surgical or therapeutic event. For example, observing any changes in measurements before a neurological surgery and after a surgery may provide valuable information about the consequence of the surgical operations on movement performance. Additionally, we can utilize a handgrip device that can measure the grip strength in a standard unit, such as Newton or kilogram. This design may provide a wider range of feature extraction functions, which allows us to perform various experiments related to disease progress over time. Our research group has successfully implemented a new handgrip design using a spring and

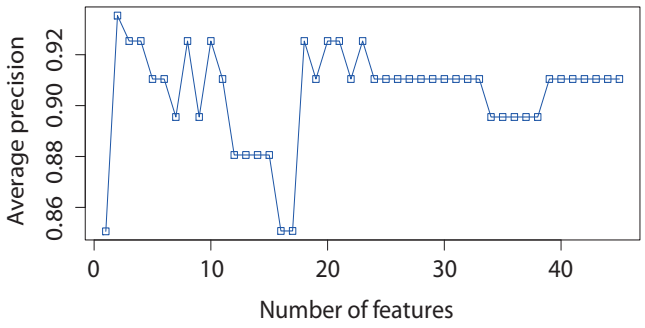

Figure 12: The average classification accuracy of GOI composed of patients with CVA over different number of features. The results show that the maximum average accuracy rate of 93.54% is achieved when the highest 2 features are employed.

a position sensor, and it is currently undergoing another set of clinical trials.

8. REFERENCES

[1] *Public health and aging: trends in aging - United States and worldwide*, volume 52. Centers for Disease Control and Prevention, 2003.

[2] Interlink Electronics, http://www.interlinkelec.com/, 2011.

[3] Texas Instruments MSP430 Microcontroller, http://www.ti.com/msp430, 2011.

[4] F. Dabiri, A. Vahdatpour, and et. al. Ubiquitous personal assistive system for neuropathy. In *The 2nd International Workshop on Systems and Networking Support for Healthcare and Assisted Living Environments (Healthnet'08) in conjunction with ACM MobiSys*, Colorado, US, 2008.

[5] E. R. Dorsey, R. Constantinescu, J. P. Thompson, and et al. Projected number of people with parkinson disease in the most populous nations, 2005 through 2030. *Neurology*, 68(5):384–386, January 2007.

[6] C. Dumont, M. Popovic, and et al. Dynamic force-sharing in multi-digit task. *Clinical Biomechanics*, 21(2):138–146, Feburary 2006.

[7] A. Fugl-Meyer, L. Jaasko, S. Olsson, and et al. The post-stroke hemiplegic patient. 1. a method for evaluation of physical performance. *Scand J Rehabil Med.*, 7(1):13–31, 1975.

[8] D. Gladstone, C. Danells, and S. Black. The fugl-meyer assessment of motor recovery after stroke: a critical review of its measurement properties. *Neurorehabil Neural Repair*, 16(3):232–240, 2002.

[9] I. Guyon and A. Elisseeff. An introduction to variable and feature selection. *Journal of Machine Learning Research*, 3:1157–1182, March 2003.

[10] R. Jafari, D. Jindrich, V. Edgerton, and M. Sarrafzadeh. Cmas: Clinical movement assessment system for neuromotor disorders. In *IEEE BioCas 2006: Biomedical Circuits and Systems Conference*, London, UK, Novermber 2006.

[11] L. H. Jakobsen, I. K. Rask, and J. Kondrup. Validation of handgrip strength and endurance as a measure of physical function and quality of life in healthy subjects and patients. *Nutrition*, 2009.

[12] R. Kohavi and G. John. Wrapper for feature subset selection. *Artificial Intelligence*, 97(1-2):273–324, 1997.

[13] S. Mazzoleni, J. V. Vaerenbergh, A. Toth, and et al. Alladin: a novel mechatronic platform for assessing post-stroke functional recovery. In *ICORR 2005: 9th Int. Conf. on Rehabilitation Robotics*, NY, USA, 2005.

[14] W. Memberg and P. Crago. Instrumented objects for quantitative evaluation of hand grasp. *J of Rehabilitation Research and Development*, 34(1):82–90, January 1997.

[15] D. Nowak and J. Hermsdorfer. Grip force behavior during object manipulation in neurological disorders: toward an objective evaluation of manual performance deficits. *Mov Discord*, 20(1):11–25, 2005.

[16] G. Pour. Ubiquitous personal assistive system for neuropathy. In *International Conference on Computational Inteligence for Modelling Control and Automation and International Conference on Intelligent Agents Web Technologies and International Commerce (CIMCA'06)*, Sydney, Australia, 2006.

[17] P. Raghavan, E. Petra1, and et al. Patterns of impairment in digit independence after subcortical stroke. *J Neurophysiol*, 95(1):269–278, 2006.

[18] M. Selzer, S. Clark, and et al. *Textbook of neural repair and rehabilitation*. Cambridge Univerrsity Press, Cambridge, UK, 2006.

[19] J. K. Shim, H. Olafsdottir, and et al. The emergence and disappearance of multi-digit synergies during force-production tasks. *Experimental Brain Research*, 164(2):260–270, July 2005.

[20] H. van Dijk, M. Jannink, and H. Hermens. Effect of augmented feedback on motor function of the affected upper extremity in rehabilitation patients: a systematic review of randomized controlled trials. *J Rehabil Med*, 37(4):202–211, July 2005.

[21] F. Vecchi, C. Freschi, and et. al. Experimental evaluation of two commercial force sensors for applications in biomechanics and motor control. In *Proc. IFESS Conf.*, Aalbor, DK, June 2000.

[22] C. Waggoner and R. LeLieuvre. A method to increase compliance to exercise regimens in rheumatoid arthritis patients. *Journal of Behavioral Medicine*, 4(2):191–201, June 1981.

[23] H. Wan, M. Sengupta, V. Velkoff, and K. DeBarrow. *U.S. Census Bureau. 65+ in the United State: 2005 Current Population Reports*. Government Printing Office, Washington DC, 2006.